

CReFT-CAD: Boosting Orthographic Projection Reasoning for CAD via Reinforcement Fine-Tuning

Ke Niu*, Zhuofan Chen*, Haiyang Yu, Yuwen Chen, Teng Fu, Mengyang Zhao, Bin Li[✉],
Xiangyang Xue[✉]

Fudan University, China
{kniu22,zfchen23,tfu23}@m.fudan.edu.cn
{hyu20,myzhao20,libin,xyxue}@fudan.edu.cn

Abstract

Computer-Aided Design (CAD) plays a pivotal role in industrial manufacturing. Orthographic projection reasoning underpins the entire CAD workflow, encompassing design, manufacturing, and simulation. However, prevailing deep-learning approaches employ standard 3D reconstruction pipelines as an alternative, which often introduce imprecise dimensions and limit the parametric editability required for CAD workflows. Recently, some researchers adopt vision-language models (VLMs), particularly supervised fine-tuning (SFT), to tackle CAD-related challenges. SFT shows promise but often devolves into pattern memorization, yielding poor out-of-distribution performance on complex reasoning tasks. To address these gaps, we introduce CReFT-CAD, a two-stage fine-tuning paradigm that first employs a curriculum-driven reinforcement learning stage with difficulty-aware rewards to build reasoning ability steadily, and then applies supervised post-tuning to hone instruction following and semantic extraction. Complementing this, we release TriView2CAD, the first large-scale, open-source benchmark for orthographic projection reasoning, comprising 200,000 synthetic and 3,000 real-world orthographic projections with precise dimension annotations and six interoperable data modalities. We benchmark leading VLMs on orthographic projection reasoning and demonstrate that CReFT-CAD substantially improves reasoning accuracy and out-of-distribution generalizability in real-world scenarios, offering valuable insights for advancing CAD reasoning research. The code and adopted datasets are available at <https://github.com/KeNiu042/CReFT-CAD>.

1 Introduction

Computer-Aided Design (CAD) is now integral to industrial product development, driving design, manufacturing, and simulation workflows. In the design phase, engineers use CAD drawings or rasterized orthographic projections for their precision and easy editability. During manufacturing, these drawings are converted into constraint-based parameter tables, and for simulation, they yield boundary-representation (B-Rep) data or textual geometry descriptions. A truly user-centric pipeline thus requires accurate semantic parsing of orthographic projection: automated extraction of parameter tables directly produces 3D models that meet stringent manufacturing and simulation standards. By contrast, existing reverse-engineering methods rely on expensive 2D/3D scanning hardware and labor-intensive post-processing, severely limiting scalability and broad industrial adoption.

With the advent of deep learning, orthographic projection reasoning has typically been cast as a standard 3D reconstruction pipeline: rasterized drawings are processed by models that output B-Rep

* Equal contribution. ✉ Corresponding authors.

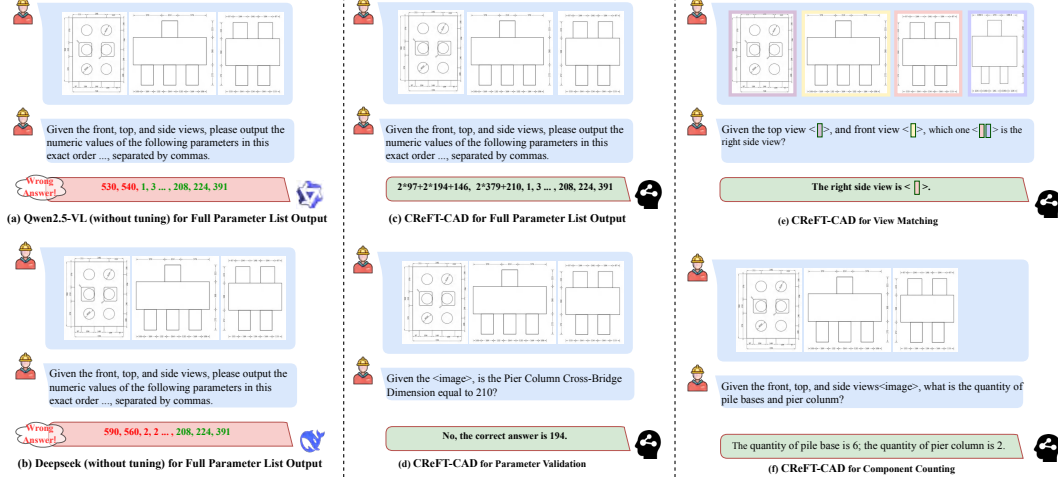


Figure 1: (a) (b) show the results of parameterization tasks of orthographic projection reasoning using Qwen2.5-VL and Deepseek without tuning. (c)–(f) illustrate CReFT-CAD’s capabilities across various orthographic projection reasoning tasks.

structures [1, 2], point clouds [3, 4], or meshes [5]. However, two critical shortcomings remain. First, **industrial drawings allow virtually zero tolerance for missing or erroneous components**: pixel-level discretization errors in reconstruction can propagate into the 3D model, causing failures in downstream manufacturing and simulation. Second, **practical CAD workflows demand parametric editability and precise semantic alignment**—capabilities that common 3D representations lack. Although some methods generate CAD command sequences to restore editability, they still overlook the nuanced semantics of orthographic views and thus fail to map 2D drawing features to their intended 3D counterparts reliably.

Recent works leverage the modality alignment and semantic reasoning strengths of vision–language models (VLMs) [6–11], applying supervised fine-tuning (SFT) to address CAD challenges [12–14]. However, orthographic projection reasoning demands genuine inferential ability, and task-specific SFT often leads to memorization and out-of-distribution (OOD) degradation rather than deeper reasoning [15]. Inspired by DeepSeek R1-Zero’s Group Relative Policy Optimization (GRPO) [16], we propose Curriculum-driven Reinforcement Fine-tuning for CAD (CReFT-CAD),

CReFT-CAD is a versatile framework that assists engineers in achieving orthographic projection reasoning throughout the entire lifecycle of industrial design, from design and manufacturing to simulation, in an interactive manner, as shown in Fig. 1. CReFT-CAD is a two-stage paradigm that combines reinforcement learning and supervised tuning. **Curriculum-driven Reinforcement Fine-tuning**: We introduce a difficulty-aware reward mechanism that incrementally escalates task complexity, gradually exposing the model to more complex reasoning challenges and promoting stable policy optimization. **Supervised Post-tuning**: Building on the reinforced model, we further refine its instruction-following and reasoning capabilities via multi-task SFT. Our qualitative and quantitative evaluations demonstrate that CReFT-CAD delivers robust orthographic projection reasoning and strong generalization in OOD scenarios. Another major obstacle in orthographic projection reasoning has been the lack of open-source datasets with high-fidelity annotations. To fill this gap, we introduce TriView2CAD, the first large-scale benchmark tailored for industrial CAD pipelines. Leveraging real-world design archives, we employ a constraint-driven synthesis pipeline to generate 200,000 synthetic and 3,000 real-world three-view sets, each annotated with precise, one-to-one dimension labels tied to their corresponding geometric primitives. This design enables models to extract quantitative measurements from rasterized drawings and enforce exact geometric constraints for simulation-ready 3D reconstruction.

2 Related Work

2.1 Orthographic projection reasoning for CAD

Understanding and reasoning with orthographic projection is a fundamental and longstanding challenge in CAD-related tasks [17–19]. With the development of 3D reconstruction methods, existing orthographic projection reasoning methods have largely focused on standard 3D reconstruction pipelines. SPARE3D [20] introduces a dataset designed to evaluate the spatial reasoning capabilities of AI systems through 2D line drawings of 3D objects. Contrastive-SPARE3D [21] propose a self-supervised binary classification network that helps to learn 3D object line drawings representations that are detail-sensitive and view-invariant. PlankAssembly [22] introduces a transformer-based sequence generation model that learns flexible mappings between inputs and outputs. IsoTGAN [23] introduces a novel Gaussian-enhanced Euclidean attention mechanism and a geometric constraint loss function to enhance local image features further. GaussianCAD [24] employs a custom sparse-view 3D reconstruction method, eliminating the reliance on vector CAD sketches and 3D real-world data.

2.2 Applications of LVLMs in CAD-Related tasks

Recent work on applying vision–language models (VLMs) to CAD tasks can be grouped into three main categories: **1) Direct Adaptation of Pretrained VLMs.** CAD-Recode [25] leverages a VLM to translate raw point-cloud inputs into executable Python code. Both LEAM [26] and LLM4CAD [27] generate CAD models by jointly leveraging textual descriptions and image inputs. CAD-Assistant [28] introduces a novel approach that leverages VLMs as planners, where the model interacts with Python APIs to accomplish various CAD tasks. **2) Supervised Fine-Tuning (SFT).** CAD2Program [12] generates 3D parametric models from 2D CAD drawings. CAD-MLLM [29] enables parametric CAD modeling from text, images, and point clouds, and proposes the Omni-CAD dataset. **3) Reinforcement Learning–Based Tunings.** RLCAD [30] proposes a reinforcement learning environment to generate complex CAD models. CADCrafter [31] presents an image-to-CAD model generation framework, fine-tuned via Direct Preference Optimization (DPO) to translate input images directly into executable CAD representations.

3 TriView2CAD: Benchmarking orthographic projection reasoning

As previously noted, a critical barrier in CAD research is the absence of an open-source dataset with high-fidelity annotations for orthographic projection reasoning. Existing benchmarks focus on 3D reconstruction from rasterized 2D views, yet diverge from real-world engineering drawing interpretation in three key aspects:

Lack of precise dimensional annotations. Existing orthographic projection benchmarks provide only rasterized drawings without precise dimension annotations. It causes models to prioritize relative scale over exact measurements, and pixel-level errors in raster images can easily propagate into the reconstructed 3D model, resulting in inaccuracies. Additionally, the limited editability of reconstructed 3D models precludes corrective adjustments during design and simulation.

Lack of explicit logical reasoning tasks. No current dataset evaluates a model’s inferential capabilities within or across orthographic views. Consequently, models trained on these benchmarks learn pixel-level reconstruction but fail to handle real-world challenges such as inferring omitted annotations or exploiting structural symmetries.

Lack of essential CAD modalities. Most datasets include only one or two modalities—typically raster images and, at best, a single 3D format (meshes or point clouds). This limits coverage omits critical data representations (e.g., parameter tables, vector CAD files, executable commands, STEP/B-Rep) needed for end-to-end CAD design, manufacturing, and simulation pipelines.

3.1 Dataset construction

In this work, we focus on prefabricated bridge piers due to their inherently modular composition of repeated, standardized components, which yields a compact yet expressive parameter space for dataset synthesis. Moreover, prefabricated piers are ubiquitous in modern infrastructure and supported by extensive archives of CAD drawings and manufacturing documentation. TriView2CAD comprises

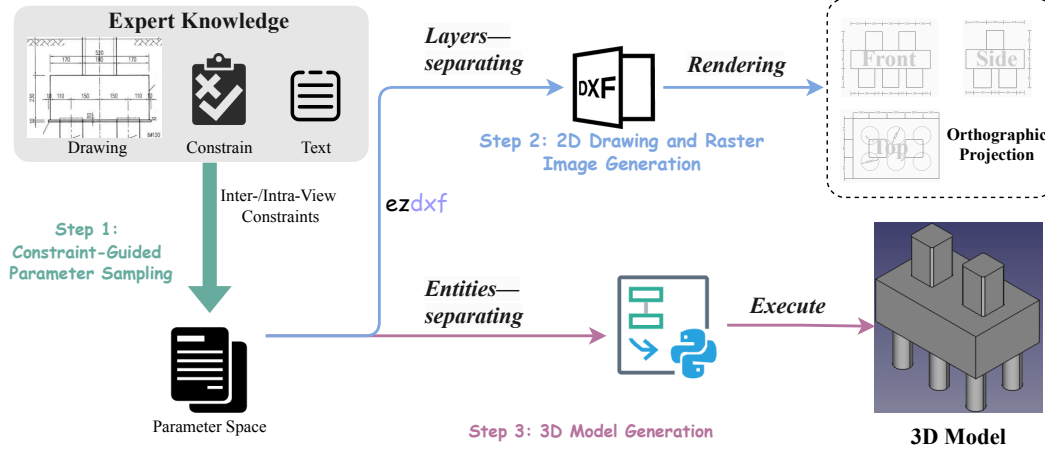


Figure 2: Constraint-driven synthesis pipeline for TriView2CAD.

200,000 synthetic samples and 3,000 real-world samples. The synthetic data are split 80/20 into training and test sets, while, due to the scarcity of real-world engineering drawings, all 3,000 real-world samples are reserved exclusively for testing. The synthetic test set is used to evaluate in-domain performance. As shown in Fig. 3, real-world images typically exhibit more complex structures, primarily due to redundant annotation lines causing occlusions, overlap with other components, and the inclusion of non-numeric annotations, serving to assess out-of-distribution generalization in authentic CAD scenarios. To mirror end-to-end industrial workflows, TriView2CAD provides six interconnected data modalities per sample—structured parameter tables (JSON), vector CAD drawings (DXF), raster images (PNG), executable modeling scripts, and two standard 3D formats (STEP and B-Rep). This comprehensive suite supports tasks from early design to downstream manufacturing and simulation. As shown in Fig. 5, we employ a constraint-driven synthesis pipeline. The detailed steps are as follows:

Step 1: Constraint-Guided Parameter Sampling We first analyze real-world CAD drawings to define a 15-dimensional parameter space subject to two constraint classes. **Intra-View Constraints** enforce both topological closure and physical validity within each projection: every component must form a gap- and overlap-free contour, and paired dimensions must satisfy domain-specific engineering constraints (e.g., “Cross-Bridge Pier Spacing” < “Cap Beam Cross-Bridge Dimension”). **Inter-View Constraints** ensure cross-projection consistency by requiring every measurement annotated in one view to exactly match its counterpart (height, width, and depth) in the other views. By embedding these constraints into our sampling pipeline, we guarantee that every synthetic design is geometrically coherent and adheres to real-world engineering practices.

Step 2: 2D Drawing and Raster Image Generation We employ the ezdxf library to translate each sampled parameter vector into a vectorized 2D CAD drawing (DXF), mapping numeric dimensions to primitives such as lines, circles, and arcs to form coherent orthographic projections. We leverage ezdxf’s layers-separating function to partition primitives into semantic layers, thereby enhancing the editability of the resulting CAD drawings. Each DXF file is then loaded into FreeCAD [32], where we capture high-resolution screenshots to produce three orthographic views (front, top, and side).

Step 3: 3D Model Generation We employ the FreeCAD Python API to reconstruct 3D model from its parameter vector. Mirroring our 2D pipeline, we decompose the model into individual entities

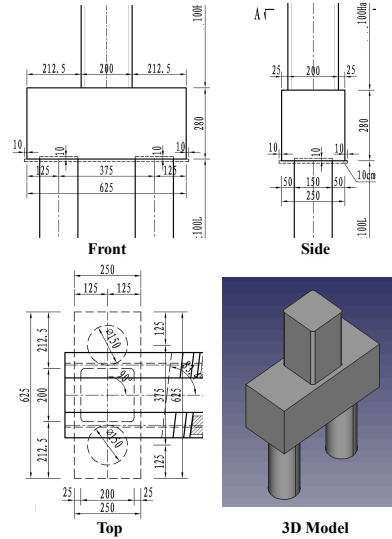


Figure 3: Examples of Real-World Orthographic Projections and its 3D model.

Training Tasks	Input Prompt	Response
Dichotomous choice task	Given the front, top, and side views, please refer to the required field names below, and determine whether the given parameter values ...match the image.	Yes/NO
Multiple choice task	Given the front, top, and side views, please refer to the required field names below, and choose all options that match the image. ...Options: A. 860, 833, ..., 356 B. 860, <mask>, ..., 356 C... D...	A/B/C/D
Parameterization task based on CoT	Given the front, top, and side views, please output only the numeric values of the following parameters in this exact order..., separated by commas.	2*82+2*188+148, 2*398+160, ..., 222

Figure 4: Diagram design of three tasks in curriculum-driven reinforcement fine-tuning.

and generate scripted commands that accurately position each primitive according to the intra- and inter-view constraints established in Step 1. By executing these scripts, we automatically produce industry-standard STEP and B-Rep files, closing the loop from parameter sampling to editable, simulation-ready CAD geometry.

3.2 Evaluation of TriView2CAD

We benchmark seven leading vision–language models on TriView2CAD to perform high-precision orthographic projection reasoning. **The evaluation results are presented in Sec. 3.2.** Reflecting real-world CAD workflows, we define three complementary evaluation tasks to rigorously test a model’s ability to extract precise dimension annotations from rasterized orthographic projection and infer the underlying geometric relationships. **(i) Dimension recognition and pairing** Models identify each annotated dimension in a single orthographic view and map it to its corresponding geometric feature. **(ii) Primitive counting** Models count instances of specified CAD elements (e.g., number of pier columns), testing their ability to parse structural composition. **(iii) Composite Parameter Computation** Models compute engineering-critical derived quantities—for example, the Cross-Bridge Pier Spacing is defined as the sum of the Pier Column Cross-Bridge Dimension and the Pile Spacing. Overall, we define a 15-dimensional parameter space comprising 6 recognition parameters, 3 counting parameters, and 6 composite calculation parameters. During evaluation, we treat each individual parameter as a separate prediction. The overall accuracy is then computed as the total number of correctly predicted parameters divided by the total number of parameters across all test samples. This evaluation suite exposes each model’s strengths and weaknesses in handling the tightly coupled semantic and quantitative demands of orthographic projection CAD reasoning.

4 Methodology

Inspired by the success of reinforcement learning–based tuning methods [33, 34], we present Progressive Reinforcement Fine-tuning for CAD (CReFT-CAD), a orthographic-projection reasoning framework. CReFT-CAD combines a ViT-based visual encoder with Qwen2.5 [35]. First, Progressive Reinforcement Fine-tuning employs a curriculum of three progressively harder reasoning tasks under a difficulty-aware reward scheme, enabling the model to move beyond rote pattern matching toward robust reasoning while improving OOD resilience. Second, Supervised Post-tuning refines the model’s instruction-following to support interactive, real-world CAD queries.

4.1 Curriculum-driven reinforcement fine-tuning

Orthographic projection reasoning is a complex reasoning task that encompasses not only dimension recognition and pairing but also primitive counting and more intricate composite parameter computation tasks. Building on GRPO, we propose a Curriculum-driven Reinforcement Fine-tuning (CReFT) strategy, which incrementally exposes the model to progressively more complex training tasks to enhance its reasoning and generalization capabilities. Our tasks design mirrors the core steps of expert engineers in verifying CAD drawings, incorporating dichotomous choice task, multiple choice task, and parameterization tasks based on chain-of-thought (CoT). For each task, we design a tailored, efficient reward function to ensure the model can steadily and stably optimize its reasoning performance.

Data engine. We leverage 160,000 image–text instruction pairs using the synthetic training set of TriView2CAD, where each prompt includes a given orthographic projection and all 15 parameter

key-value pairs, as shown in Fig. 4. To ensure a balanced training signal across all three tasks, 50% of the training responses are entirely correct, while the remaining 50% contain errors of varying magnitude. Specifically, for the dichotomous choice task, we ensure that each negative response contains n erroneous parameter values, where n follows a uniform distribution $N \sim \text{Uniform}(a, b)$, where $a = 1$ and $b = 15$.

For the multiple choice task, p parameter values are masked in each image-text instruction pair. The masking mechanism ensures the diversity of options. This approach prevents the model from simply deriving the answer through parameterization, bypassing the complex multiple choice reasoning required in the task. Instead, it forces the model to engage in decision-making actively, considering multiple potential solutions and selecting the correct responses based on a deeper understanding. For each instruction pair, unmasked values are correct, while for the incorrect parameter value lists, all unmasked values, except for randomly selected q erroneous lists. Both the masked values p and the number of incorrect values q follow a normal distribution, introducing a smooth and gradual variation in the difficulty of the learning task. This variation helps the model to learn in a more structured and progressive manner.

For the parameterization task, we construct image-text instruction pairs based on Chain-of-Thought (CoT) reasoning. Specifically, as for Composite Parameter Computation, expert knowledge guides the model through a step-by-step reasoning guidance to arrive at the correct output. The step-by-step workflow of reasoning guidance is as follow: 1) recognize parameters required for the computation of the composite parameter; 2) provide the calculation formula for the composite parameter; 3) generate the predicted result based on the formula and the factor parameters

Training strategy. Given that our task involves highly customized inputs and outputs rather than a general-purpose problem, directly applying a pretrained VLM for reasoning tasks and generating required outputs proves ineffective. As a result, the model cannot effectively execute the reinforcement learning reward mechanism, as the reward will always be 0. To address this, prior to executing each training task, we pre-sample a subset of image-text instruction pairs to "warm up" the model, facilitating the initialization of the reinforcement learning (RL) reward mechanism.

4.1.1 Task 1: Dichotomous choice task

As for this task, the model's output is constrained to dichotomous responses, either "yes" or "no." A "yes" answer is given only when the entire 15-dimensional parameter space is completely correct, while any error, even in a single parameter, results in a "no" response. This strict criterion ensures that the model is incentivized to produce fully accurate parameterizations. To align with this setup, the reward function is defined as follows:

$$R_{p1} = \begin{cases} 1, & \text{if all parameters are correct} \\ 0, & \text{otherwise} \end{cases} \quad (1)$$

4.1.2 Task 2: Multiple choice task

Training strategy. In the task 2, we introduce multiple choice tasks to further increase the complexity of decision-making. These tasks require the model to select from multiple parameter value lists, which significantly enhancing the cognitive load compared to binary decisions. Building on the first stage, we pre-sample a subset of image-text instruction pairs to perform instruction-following training on the LLM. This training allows the model to generate structured outputs in the form of multiple choice questions, enabling the reinforcement learning reward mechanism. Additionally, we designed a stringent reward function that encourages the model to maximize the utilization of image-text instruction pairs, ensuring that it extracts and applies all relevant information from both the visual and textual components. The reward function incentivizes the model to select the most accurate option from the provided set of choices. Any incorrect selection results in a reward of 0, thereby pushing the model to focus on precision and reliability in its decision-making process.

Let S_{correct} be the set of correct parameter value lists, $S_{\text{incorrect}}$ be the set of incorrect parameter value lists, and S_{Selected} be the set of selected parameter value lists by the model. The reward function R_{p2}

is defined as:

$$R_{p2} = \begin{cases} 1 & \text{if } S_{\text{selected}} = S_{\text{correct}} \\ 0.2 & \text{if } S_{\text{selected}} \supseteq S_{\text{correct}} \text{ but } S_{\text{selected}} \neq S_{\text{correct}} \\ 0 & \text{if } (S_{\text{selected}} \cap S_{\text{correct}} \neq \emptyset) \text{ and } (S_{\text{selected}} \cap S_{\text{incorrect}} \neq \emptyset) \\ 0 & \text{if } S_{\text{selected}} = S_{\text{incorrect}} \end{cases} \quad (2)$$

Where $S_{\text{Selected}} = S_{\text{correct}}$ means the model selects only the correct parameter value lists; $S_{\text{Selected}} \supseteq S_{\text{correct}}$ but $S_{\text{Selected}} \neq S_{\text{correct}}$ means the model selects all correct lists but fails to select all of them; $S_{\text{Selected}} \cap S_{\text{correct}} \neq \emptyset$ and $S_{\text{Selected}} \cap S_{\text{incorrect}} \neq \emptyset$ means the model selects both correct and incorrect parameter value lists; $S_{\text{Selected}} = S_{\text{incorrect}}$ means the model selects incorrect parameter value lists.

4.1.3 Task 3: Parameterization tasks based on chain-of-thought

Training strategy. In the training process, we begin with the model trained in task 2, and sample synthetic data to construct standard orthographic projection reasoning question-answer pairs. These pairs are then used to perform small-batch fine-tuning. Once the model is fine-tuned, we assess the difficulty of predicting the 15-dimensional parameters by evaluating the model’s performance on a test set. The prediction accuracy for each parameter is categorized into three difficulty levels: **Easy Attributes:** Attributes with an accuracy greater than 0.8. **Medium Attributes:** Attributes with accuracy between 0.2 and 0.8. **Difficult Attributes:** Attributes with accuracy less than 0.2. This difficulty classification is then used to design the reward function. The reward for each correctly answered attribute is determined by its difficulty level as follows:

$$R_{p3} = \begin{cases} 1 & \text{if the model correctly predicts an easy attribute} \\ 1.5 & \text{if the model correctly predicts a medium attribute} \\ 2 & \text{if the model correctly predicts a hard attribute} \\ 0 & \text{if the model’s prediction is incorrect} \end{cases} \quad (3)$$

This reward function ensures that the model is motivated to gradually improve across all difficulty levels, with greater emphasis on mastering the more challenging tasks, thus enhancing the model’s overall reasoning capabilities in orthographic projection tasks.

4.2 Supervised post-tuning

After the CReFT stage, where the model developed robust reasoning and generalization capabilities, the focus of the Supervised Post-tuning task shifts to enhancing the model’s instruction-following ability. During this stage, we rethink the industrial design application context and, with a user-centric approach, reformulate tasks in the style of Visual Question Answering (VQA). By leveraging multimodal language models, we design specific tasks that guide the model to output a comprehensive list of parameters and make critical judgments based on orthographic projection. In this stage, the model is trained to process the following tasks: **1) Full Parameter List Output Task:** The goal is to generate a fully accurate set of parameter key-value pairs, which is the most common format for outputs during the simulation phase. **2) Parameter Validation Task:** The task is to compare the extracted parameter key-value pairs with the accurate parameter key-value pairs in the orthographic projection to determine whether the extracted parameters are correct. **3) View Matching Task:** The model is given two individual orthographic projection views. The model must, based on parameter constraints and rasterized images, assess whether the views correspond to the same overall 3D object or design. **4) Component Counting Task:** The model is required to identify and count specific components in the drawing, such as bridge piers or columns, based on the given parameter constraints. The output of this task helps to quantify the number of elements in the design, aiding in material estimation and component verification.

By employing this post-tuning phase, we enhance the model’s ability to interpret and respond to complex design queries, thereby improving its interactive reasoning abilities and making it more applicable to real-world industrial design workflows.

Table 1: Performance comparison of various VLMs on orthographic projection reasoning tasks.

PROMPTS	Without Reasoning Guidance				Reasoning Guidance			
	Test Img	+Reference Img	+Answered Pair	+Attribute Explanation	Test Img	+Reference Img	+Answered Pair	+Attribute Explanation
Phi-3.5-Vision [36]	4.22	8.95	8.05	6.26	11.32	14.40	16.16	15.79
LLaVA-OneVision [37]	9.16	16.06	15.65	14.84	9.10	16.81	16.21	20.53
DeepSeek-VL [38]	8.16	22.68	20.03	12.65	14.02	20.31	24.62	25.45
InternVL2.5 [39]	15.79	18.82	23.30	17.16	15.63	22.35	24.47	23.73
InternVL3 [39]	15.46	17.90	22.44	17.91	15.81	21.98	23.58	17.05
Qwen2.5-Omni [40]	23.43	28.89	28.74	26.50	26.12	30.93	29.40	35.71
Qwen2.5-VL [41]	24.54	30.76	30.47	25.86	24.54	32.78	33.64	38.88
Ours	80.86	82.99	83.24	82.67	81.35	83.11	82.87	84.03

5 Experiments

Implementation Details. All experiments are conducted on NVIDIA A100 GPUs. Most experiments use GOT-OCR2.0 as the base model, trained on a single server equipped with 8 A100 GPUs and a batch size of 64. We use the AdamW optimizer with a cosine annealing scheduler. The hyperparameters are configured as follows: (1) Learning rate: $1e-6$ for RL (GRPO) training and $2e-5$ for baseline SFT experiments. (2) Maximum input image size: 2,483,776 pixels. (3) Total GRPO training steps: 1500.

Datasets and Metrics. We evaluate both the leading vision–language models (VLMs) and the proposed method on TriView2CAD, following the evaluation strategy outlined in Sec. 3.2. The synthetic test set is used to assess in-domain accuracy. Due to the difficulty in obtaining real-world data, all 3,000 real-world samples are reserved exclusively for testing, allowing us to evaluate out-of-distribution (OOD) generalization in real-world scenarios.

We design four distinct prompt configurations to probe their orthographic projection reasoning capabilities: **Test image-Only**: Models receive only the target rasterized drawings. **Test image + Reference Image**: In addition to the target drawings, models are given a reference image—rendered on the same geometry layer—with all dimension names to supply semantic alignment. **Test image + Answered Pair**: Inputs consist of the target drawings plus a correctly paired raster image and its parameter vector, providing an exemplar mapping between visual features and quantitative parameters. **Test image + Attribute Explanation**: Models are supplied with the target drawings alongside a detailed textual interpretation authored by professional engineers.

Given that orthographic projection reasoning involves complex multi-step inference and current pretrained VLMs limit exposure to CAD drawings, we incorporate explicit reasoning guidance into each prompt format to encourage clear reasoning trajectories. For each of the four different prompt input formats, we outline detailed step-by-step instructions for completing the task. These steps are designed to guide the model through the reasoning process in a structured manner. The complete set of instructions for each format is provided in the supplementary materials.

5.1 Performance on in-domain test set.

The experimental results, as shown in Tab. 3, demonstrate that our method significantly outperforms existing VLMs on orthographic projection reasoning tasks across all prompt formats. Specifically, in the Without Reasoning Guidance setting, the "+Answered Pair" prompt achieves the highest accuracy of 83.24%. In the Reasoning Guidance setting, our model achieves an accuracy of 84.03% in the "+Attribute Explanation" prompt. Furthermore, our method exhibits strong performance even in the "Test Image Only" condition, where we achieve 80.86%. This improvement highlights the effectiveness of our approach.

It is worth noting that the performance improvement from "without reasoning guidance" to "with reasoning guidance" is not as significant. This is primarily because, through our CReFT approach, the model learns effective reasoning strategies via the difficulty-aware reward mechanism, thereby reducing the need for additional guidance to achieve further significant gains. Based on our benchmarking of the seven leading VLMs, we present several important findings, as follows: **1) This reasoning task**

remains a tough challenge for pretrained VLMs. Overall, orthographic projection reasoning entails not only reading textual dimensions and visual features, but also matching annotations to geometry primitives, counting structural elements, and computing composite parameters. **2) Different prompt formats influence the performance.** In both the Without Reasoning Guidance and With Reasoning Guidance settings, different prompt formats lead to varying degrees of performance improvement. **3)Introducing reasoning guidance yields consistent gains across all seven VLMs.** Introducing appropriate reasoning guidance significantly enhances the model’s ability to perform reasoning tasks effectively. Further analysis regarding the three findings are presented in the supplementary materials.

5.2 Performance on real-world test set.

We utilize all 3,000 real-world samples to evaluate out-of-distribution (OOD) generalization in real-world scenarios. The baseline model, Qwen2.5-VL, achieves an accuracy of 13.47%, which is lower than its performance on synthetic data (24.54%). This performance drop is primarily due to the more complex structure and occlusion relationships present in the real-world data, as discussed in Sec. 3.1, which increases the difficulty of the task. We also compare the results with a model trained using a SFT strategy, which achieve an accuracy of 36.15%. This improvement can be attributed to significant gains in Primitive Counting tasks. However, the model still struggle with Composite Parameter Computation, highlighting the limitations of traditional SFT. Our method, using CReFT, achieves an accuracy of 46.67%, demonstrating that our method can effectively address OOD generalization and lead to significant improvements on more complex real-world data.

5.3 Abalation study

With CoT VS without CoT. The results from Tab. 2 reveal a significant improvement in performance when incorporating chain-of-thought (CoT) reasoning. Specifically, the accuracy for individual Task 3 increase from 46.16% to 74.15% after adding CoT , demonstrating a clear performance boost. When combining multiple training tasks, such as Task 1 + Task 3 and Task 2 + Task 3, the improvements are even more pronounced, with accuracies reaching 77.90% and 67.75%, respectively. The most notable enhancement is observed in the combination of Task 1 + Task 2 + Task 3, where the accuracy increases from 46.24% to 81.35%. The primary source of these improvements lies in how CoT helps break down complex Composite Parameter Computation tasks into more manageable, incremental steps. The CoT mechanism, however, guides the model through each individual component of the computation, allowing for a step-by-step approach that improves the model’s reasoning capability.

Table 2: Ablation study results.

METHOD	w/o CoT	with CoT
Task3	46.16	74.15
Task1 + Task3	46.05	77.90
Task2 + Task3	30.71	67.75
Task1 + Task2 + Task3	46.24	81.35

Three training tasks. Notably, in the CoT setting, combining Task 1 and Task 3 provides a performance boost, increasing accuracy from 74.15% to 77.90%. However, when Task 2 is added, the model’s performance decreases. This decline can be attributed to the design of Task 2, which includes a substantial number of masked elements within the instruction data. By exposing the model to higher uncertainty, Task 2 forces the model to contend with incomplete or ambiguous information, which ultimately hinders its ability to perform effectively on the task. On the other hand, when all three tasks (Task 1 + Task 2 + Task 3) are used together, the model’s reasoning ability is fully activated, resulting in a significant performance improvement. In contrast, in the without CoT setting, the model’s performance is constrained by its inability to effectively handle multi-step reasoning tasks, where even the best-performing task combination achieves a maximum accuracy of only 46.24%.

6 Conclusion and Limitation

In this work, we address challenges in orthographic projection reasoning for Computer-Aided Design (CAD) by proposing CReFT-CAD, an innovative two-stage fine-tuning paradigm. We demonstrated that the integration of curriculum-driven reinforcement learning (RL) with difficulty-aware rewards effectively enhances the model’s reasoning ability. To further advance the field, we introduce TriView2CAD, the first large-scale, open-source benchmark specifically designed for

orthographic projection reasoning. With its comprehensive dataset of 200,000 synthetic and 3,000 real-world samples, each annotated with precise dimensions and accompanied by six interoperable data modalities. In conclusion, this work lays the groundwork for more robust, scalable solutions to CAD-related challenges, providing both a novel training paradigm and a rich dataset that can foster future research and innovation in the field.

Limitation. The accuracy on complex real-world scenarios has not yet reached a very high level. As such, the model’s generalization ability remains a key area for further development. In future work, we plan to explore techniques to enhance the model’s robustness and adaptability.

References

- [1] Karl DD Willis, Pradeep Kumar Jayaraman, Joseph G Lambourne, Hang Chu, and Yewen Pu. Engineering sketch generation for computer-aided design. In *Proceedings of the IEEE/CVF conference on computer vision and pattern recognition*, pages 2105–2114, 2021.
- [2] Xianghao Xu, Wenzhe Peng, Chin-Yi Cheng, Karl DD Willis, and Daniel Ritchie. Inferring cad modeling sequences using zone graphs. In *Proceedings of the IEEE/CVF conference on computer vision and pattern recognition*, pages 6062–6070, 2021.
- [3] Weijian Ma, Shuaiqi Chen, Yunzhong Lou, Xueyang Li, and Xiangdong Zhou. Draw step by step: Reconstructing cad construction sequences from point clouds via multimodal diffusion. In *Proceedings of the IEEE/CVF Conference on Computer Vision and Pattern Recognition*, pages 27154–27163, 2024.
- [4] Rundt Wu, Chang Xiao, and Changxi Zheng. Deepcad: A deep generative network for computer-aided design models. In *Proceedings of the IEEE/CVF International Conference on Computer Vision*, pages 6772–6782, 2021.
- [5] Long Zhang, Jianwei Guo, Jun Xiao, Xiaopeng Zhang, and Dong-Ming Yan. Blending surface segmentation and editing for 3d models. *IEEE Transactions on Visualization and Computer Graphics*, 28(8):2879–2894, 2020.
- [6] Haiyang Yu, Jinghui Lu, Yanjie Wang, Yang Li, Han Wang, Can Huang, and Bin Li. Eve: Towards end-to-end video subtitle extraction with vision-language models. *arXiv preprint arXiv:2503.04058*, 2025.
- [7] Ke Niu, Haiyang Yu, Xuelin Qian, Teng Fu, Bin Li, and Xiangyang Xue. Synthesizing efficient data with diffusion models for person re-identification pre-training. *Machine Learning*, 114(3):1–25, 2025.
- [8] Teng Fu, Xiaocong Wang, Haiyang Yu, Ke Niu, Bin Li, and Xiangyang Xue. Denoising-mot: Towards multiple object tracking with severe occlusions. In *Proceedings of the 31st ACM International Conference on Multimedia*, pages 2734–2743, 2023.
- [9] Teng Fu, Haiyang Yu, Ke Niu, Bin Li, and Xiangyang Xue. Foundation model driven appearance extraction for robust multiple object tracking. In *Proceedings of the AAAI Conference on Artificial Intelligence*, volume 39, pages 3031–3039, 2025.
- [10] Ke Niu, Haiyang Yu, Mengyang Zhao, Teng Fu, Siyang Yi, Wei Lu, Bin Li, Xuelin Qian, and Xiangyang Xue. Chatreid: Open-ended interactive person retrieval via hierarchical progressive tuning for vision language models. *arXiv preprint arXiv:2502.19958*, 2025.
- [11] Haiyang Yu, Siyang Yi, Ke Niu, Minghan Zhuo, and Bin Li. Umit: Unifying medical imaging tasks via vision-language models. *arXiv preprint arXiv:2503.15892*, 2025.
- [12] Xilin Wang, Jia Zheng, Yuanchao Hu, Hao Zhu, Qian Yu, and Zihan Zhou. From 2d cad drawings to 3d parametric models: A vision-language approach. *arXiv preprint arXiv:2412.11892*, 2024.
- [13] Haocheng Yuan, Jing Xu, Hao Pan, Adrien Bousseau, Niloy J Mitra, and Changjian Li. Cadtalk: An algorithm and benchmark for semantic commenting of cad programs. In *Proceedings of the IEEE/CVF Conference on Computer Vision and Pattern Recognition*, pages 3753–3762, 2024.
- [14] Ke Niu, Yuwen Chen, Haiyang Yu, Zhuofan Chen, Xianghui Que, Bin Li, and Xiangyang Xue. Phtcad: Efficient cad parametric primitive analysis with progressive hierarchical tuning. *arXiv preprint arXiv:2503.18147*, 2025.
- [15] Martin Arjovsky. *Out of distribution generalization in machine learning*. PhD thesis, New York University, 2020.

- [16] Daya Guo, Dejian Yang, Haowei Zhang, Junxiao Song, Ruoyu Zhang, Runxin Xu, Qihao Zhu, Shirong Ma, Peiyi Wang, Xiao Bi, et al. Deepseek-r1: Incentivizing reasoning capability in llms via reinforcement learning. *arXiv preprint arXiv:2501.12948*, 2025.
- [17] Masanori Idesawa. A system to generate a solid figure from three view. *Bulletin of JSME*, 16(92):216–225, 1973.
- [18] Weidong Wang and Georges G Grinstein. A survey of 3d solid reconstruction from 2d projection line drawings. In *Computer Graphics Forum*, volume 12, pages 137–158. Wiley Online Library, 1993.
- [19] Byeong-Seok Shin and Yeong Gil Shin. Fast 3d solid model reconstruction from orthographic views. *Computer-Aided Design*, 30(1):63–76, 1998.
- [20] Wenyu Han, Siyuan Xiang, Chenhui Liu, Ruoyu Wang, and Chen Feng. Spare3d: A dataset for spatial reasoning on three-view line drawings. In *Proceedings of the IEEE/CVF Conference on Computer Vision and Pattern Recognition*, pages 14690–14699, 2020.
- [21] Siyuan Xiang, Anbang Yang, Yanfei Xue, Yaoqing Yang, and Chen Feng. Contrastive spatial reasoning on multi-view line drawings. *CoRR*, 2021.
- [22] Wentao Hu, Jia Zheng, Zixin Zhang, Xiaojun Yuan, Jian Yin, and Zihan Zhou. Plankassembly: Robust 3d reconstruction from three orthographic views with learnt shape programs. In *Proceedings of the IEEE/CVF International Conference on Computer Vision*, pages 18495–18505, 2023.
- [23] Thao Nguyen Phuong, Vinh Nguyen Duy, and Hidetomo Sakaino. Isotgan: Spatial and geometrical constraints at gan and transformer for 3d contour generation. In *Proceedings of the Asian Conference on Computer Vision*, pages 435–452, 2024.
- [24] Zheng Zhou, Zhe Li, Bo Yu, Lina Hu, Liang Dong, Zijian Yang, Xiaoli Liu, Ning Xu, Ziwei Wang, Yonghao Dang, et al. Gaussiand: Robust self-supervised cad reconstruction from three orthographic views using 3d gaussian splatting. *arXiv preprint arXiv:2503.05161*, 2025.
- [25] Danila Rukhovich, Elona Dupont, Dimitrios Mallis, Kseniya Cherenkova, Anis Kacem, and Djamila Aouada. Cad-recode: Reverse engineering cad code from point clouds. *arXiv preprint arXiv:2412.14042*, 2024.
- [26] Tao Wu, Kexue Fu, Qiang Hua, Xinxin Liu, Muhammad Ali Imran, and Bo Liu. Leam: A prompt-only large language model-enabled antenna modeling method. *arXiv preprint arXiv:2504.18271*, 2025.
- [27] Xingang Li, Yuewan Sun, and Zhenghui Sha. Llm4cad: Multimodal large language models for three-dimensional computer-aided design generation. *Journal of Computing and Information Science in Engineering*, 25(2), 2025.
- [28] Dimitrios Mallis, Ahmet Serdar Karadeniz, Sebastian Cavada, Danila Rukhovich, Niki Foteinopoulou, Kseniya Cherenkova, Anis Kacem, and Djamila Aouada. Cad-assistant: Tool-augmented vlms as generic cad task solvers? *arXiv preprint arXiv:2412.13810*, 2024.
- [29] Jingwei Xu, Chenyu Wang, Zibo Zhao, Wen Liu, Yi Ma, and Shenghua Gao. Cad-mllm: Unifying multimodality-conditioned cad generation with mllm. *arXiv preprint arXiv:2411.04954*, 2024.
- [30] Xiaolong Yin, Xingyu Lu, Jiahang Shen, Jingzhe Ni, Hailong Li, Ruofeng Tong, Min Tang, and Peng Du. Rlcad: Reinforcement learning training gym for revolution involved cad command sequence generation. *arXiv preprint arXiv:2503.18549*, 2025.
- [31] Cheng Chen, Jiacheng Wei, Tianrun Chen, Chi Zhang, Xiaofeng Yang, Shangzhan Zhang, Bingchen Yang, Chuan-Sheng Foo, Guosheng Lin, Qixing Huang, et al. Cadrafter: Generating computer-aided design models from unconstrained images. *arXiv preprint arXiv:2504.04753*, 2025.
- [32] Juergen Riegel, Werner Mayer, and Yorik van Havre. Freecad. *Freecadspec2002. pdf*, 2016.
- [33] Huilin Deng, Ding Zou, Rui Ma, Hongchen Luo, Yang Cao, and Yu Kang. Boosting the generalization and reasoning of vision language models with curriculum reinforcement learning. *arXiv preprint arXiv:2503.07065*, 2025.
- [34] Xinhao Li, Ziang Yan, Desen Meng, Lu Dong, Xiangyu Zeng, Yinan He, Yali Wang, Yu Qiao, Yi Wang, and Limin Wang. Videochat-r1: Enhancing spatio-temporal perception via reinforcement fine-tuning. *arXiv preprint arXiv:2504.06958*, 2025.

- [35] An Yang, Baosong Yang, Beichen Zhang, Binyuan Hui, Bo Zheng, Bowen Yu, Chengyuan Li, Dayiheng Liu, Fei Huang, Haoran Wei, et al. Qwen2. 5 technical report. *arXiv preprint arXiv:2412.15115*, 2024.
- [36] Marah Abdin, Jyoti Aneja, Hany Awadalla, Ahmed Awadallah, Ammar Ahmad Awan, Nguyen Bach, Amit Bahree, Arash Bakhtiari, Jianmin Bao, Harkirat Behl, et al. Phi-3 technical report: A highly capable language model locally on your phone. *arXiv preprint arXiv:2404.14219*, 2024.
- [37] Bo Li, Yuanhan Zhang, Dong Guo, Renrui Zhang, Feng Li, Hao Zhang, Kaichen Zhang, Yanwei Li, Ziwei Liu, and Chunyuan Li. Llava-onevision: Easy visual task transfer, 2024. URL <https://arxiv.org/abs/2408.03326>.
- [38] Haoyu Lu, Wen Liu, Bo Zhang, Bingxuan Wang, Kai Dong, Bo Liu, Jingxiang Sun, Tongzheng Ren, Zhuoshu Li, Yaofeng Sun, Chengqi Deng, Hanwei Xu, Zhenda Xie, and Chong Ruan. Deepseek-vl: Towards real-world vision-language understanding, 2024.
- [39] Zhe Chen, Jiannan Wu, Wenhai Wang, Weijie Su, Guo Chen, Sen Xing, Muyan Zhong, Qinglong Zhang, Xizhou Zhu, Lewei Lu, et al. Internvl: Scaling up vision foundation models and aligning for generic visual-linguistic tasks. In *Proceedings of the IEEE/CVF Conference on Computer Vision and Pattern Recognition*, pages 24185–24198, 2024.
- [40] Daya Guo, Dejian Yang, Haowei Zhang, Junxiao Song, Ruoyu Zhang, et al. Qwen2.5-omni technical report. *arXiv preprint arXiv:2503.20215*, 2025.
- [41] Qwen Team. Qwen2.5-vl, January 2025. URL <https://qwenlm.github.io/blog/qwen2.5-vl/>.
- [42] Peng Wang, Shuai Bai, Sinan Tan, Shijie Wang, Zhihao Fan, Jinze Bai, Keqin Chen, Xuejing Liu, Jialin Wang, Wenbin Ge, et al. Qwen2-vl: Enhancing vision-language model’s perception of the world at any resolution. *arXiv preprint arXiv:2409.12191*, 2024.

A The complete reasoning guidance for each input format

For the Test Image-Only format:

- Identify all annotated numbers in the orthographic projection, including dimensions, spacing, and height.
- Interpret their meanings based on position, orientation, and surrounding context.
- Directly assign values to some parameters, count graphical elements for quantity parameters, and compute spacing parameters based on position.

For the +Reference Image format:

- Use the reference template to understand the correspondence between primitive and parameters, and identify annotated numbers in the target image.
- Assign parameters based on position and template primitive, counting graphical primitive for quantities.
- Calculate parameters based on positional relationships or template definitions, and output the full set of parameter values.

For the +Answered Image format:

- Learn the correspondence between structures and parameters from the example image.
- Identify and interpret annotated numbers in the target image, considering their position and similarity to the example.
- Assign values to parameters, count graphical primitive for quantities, calculate parameters, and apply necessary constraints to produce final results.

For the +Attribute Explanation format:

- Clarify parameter definitions and their geometric meanings, including component types and their properties.
- Identify annotated numbers in the orthographic projection and infer their corresponding parameters.
- Assign values to parameters, compute quantities, derive spacing values from positional relationships, and output the complete parameter set with necessary constraints.

B Further analysis regarding the three findings

Table 3: Performance comparison of various VLMs on orthographic projection reasoning tasks.

PROMPTS	Without Reasoning Guidance				Reasoning Guidance			
	Test Img	+Reference Img	+Answered Pair	+Attribute Explanation	Test Img	+Reference Img	+Answered Pair	+Attribute Explanation
Phi-3.5-Vision	4.22	8.95	8.05	6.26	11.32	14.40	16.16	15.79
LLaVA-OneVision	9.16	16.06	15.65	14.84	9.10	16.81	16.21	20.53
DeepSeek-VL	8.16	22.68	20.03	12.65	14.02	20.31	24.62	25.45
InternVL2.5	15.79	18.82	23.30	17.16	15.63	22.35	24.47	23.73
InternVL3	15.46	17.90	22.44	17.91	15.81	21.98	23.58	17.05
Qwen2.5-Omni	23.43	28.89	28.74	26.50	26.12	30.93	29.40	35.71
Qwen2.5-VL	24.54	30.76	30.47	25.86	24.54	32.78	33.64	38.88
Ours	80.86	82.99	83.24	82.67	81.35	83.11	82.87	84.03

1) Remains a Tough Challenge for pretrained VLMs. Tab. 3 reports performance across four prompt formats without and with reasoning guidance. Overall, orthographic projection reasoning entails not only reading textual dimensions and visual features, but also matching annotations to geometry primitives, counting structural elements, and computing composite parameters. Consequently,

none of the off-the-shelf models fully masters this composite task. Qwen2.5-VL [42] achieves the highest accuracy—38.88% under reasoning guidance with the Test Image + Attribute Explanation prompt. This improvement stems primarily from its superior ability to parse geometry layers and read dimension labels. Crucially, its performance on reasoning-intensive parameters remains low. These findings underscore that orthographic projection CAD cannot be solved by prompting alone and requires dedicated fine-tuning strategy.

2) Prompt Format–Dependent Performance Gains. Appending an Attribute Explanation to the Test Image consistently boosts accuracy compared to the image-only baseline, with an average increase of 3 to 4 percentage points across models. This demonstrates that strong text encoders can leverage detailed, engineer-authored descriptions to guide complex geometric and numerical inferences. Similarly, providing a Reference Image or an Answered Pair results in comparable improvements, with a 4 to 5 percentage point increase in accuracy. These exemplars offer explicit visual-textual templates, simplifying the task of matching primitives to their corresponding semantic labels and dimensions. In contrast, using raw images forces models to address both perception and reasoning simultaneously, leading to the lowest performance. Collectively, these findings indicate that multimodal exemplars can enhance existing VLMs’ ability to reason over orthographic projection. However, this further underscores that additional fine-tuning strategies are crucial to fully bridging the remaining performance gap.

3)Introducing reasoning guidance yields consistent gains across all seven VLMs. Introducing reasoning guidance demonstrates that step-wise reasoning guidance helps models better decompose the multi-step orthographic projection tasks. In the absence of reasoning guidance, visual exemplar prompts (+Reference Image and +Answered Pair) deliver the largest relative improvements. However, when reasoning guidance is added, the Attribute Explanation prompt shows the greatest uplift. It stems from reasoning guidance is textual form, which synergizes most effectively with textual inputs. Hence, models with stronger text encoders (e.g., DeepSeek-V1) exhibit disproportionately larger boosts. These results underscore the necessity of integrating structured reasoning guidance to advance orthographic projection CAD reasoning.

C More performance on in-domain test set

Table 4: Performance comparison of training-free model, SFT model, and our GRPO-based model on orthographic projection reasoning tasks.

PROMPTS	Without Reasoning Guidance				Reasoning Guidance			
	Test Img	+Reference Img	+Answered Pair	+Attribute Explanation	Test Img	+Reference Img	+Answered Pair	+Attribute Explanation
Qwen2.5-VL	24.54	30.76	30.47	25.86	24.54	32.78	33.64	38.88
Qwen2.5-VL(SFT)	76.33	79.50	77.12	78.64	76.42	76.78	77.20	80.30
Ours	80.86	82.99	83.24	82.67	81.35	83.11	82.87	84.03

Tab. 4 presents the performance in-domain test set. The first row (Qwen2.5-VL) represents a training-free baseline, which exhibits consistently poor performance across all settings, indicating the inherent difficulty of this reasoning task without any fine-tuning or adaptation. The second row (Qwen2.5-VL with SFT) demonstrates a significant performance improvement, particularly when provided with reference images, answered pairs, and attribute explanations. However, despite these gains, the model still suffers from notable drops in more complex reasoning tasks, especially those involving composite parameter computation. In contrast, our method consistently outperforms both baselines across all settings, achieving the highest accuracy in all prompt configurations, with particularly strong results under reasoning guidance. These results validate the effectiveness of our approach in handling complex geometric reasoning and highlight its robustness across both simple and compositional inference scenarios.

D Failure cases and analysis

As illustrated in Fig. 5, we present four distinct failure cases, each highlighting different types of errors that can occur during the 3D model reconstruction process due to incorrect 2D parameterization.

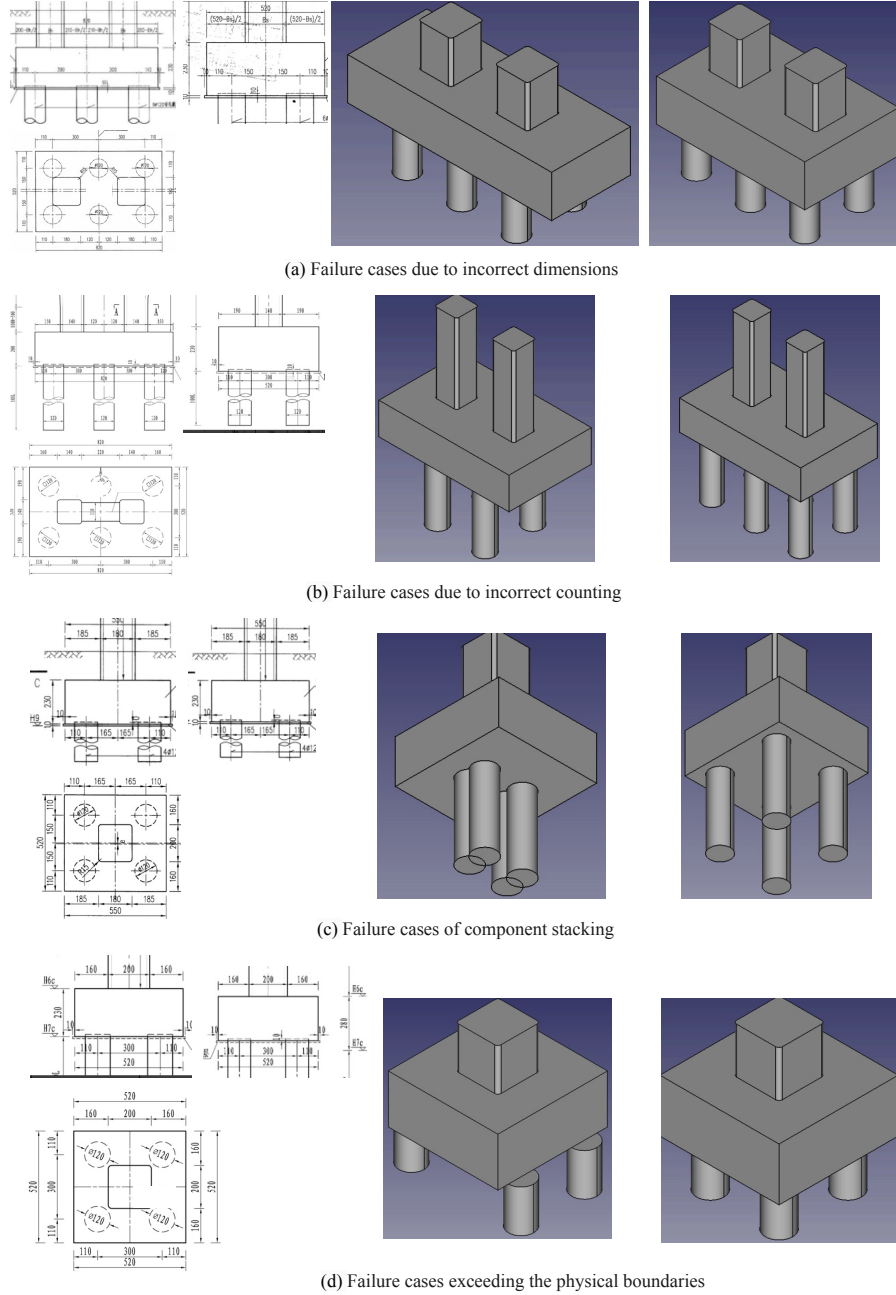


Figure 5: Four sets of failure cases. Each set consists of three parts: the left part shows the orthographic projection, the middle part presents the failed 3D model construction, and the right part illustrates the correctly constructed 3D model.

Fig. 5(a) demonstrates the error induced by incorrect dimensional parameters. Specifically, due to errors in the parameterization of certain dimensions, the constructed 3D model exhibits significant scaling issues, leading to a distorted and non-accurate representation. This failure emphasizes the critical importance of precise dimensional input when translating from 2D projections to 3D models, as even minor errors in size parameters can drastically affect the final output. Fig. 5(b) illustrates a failure caused by incorrect counting, which results in an incorrect number of primitives being identified and subsequently integrated into the 3D model. The discrepancy in the number of primitives

reflects the direct impact that improper counting and recognition of geometric elements can have on the success of the 3D reconstruction. In Fig. 5(c), we observe a stacking issue caused by errors in the calculation of composite parameters. The failure manifests as improper alignment of components in the final model, where parts of the 3D structure fail to align correctly with each other. Lastly, Fig. 5(d) shows a failure resulting from exceeding physical boundaries due to incorrect composite parameter calculations. In this case, the incorrect parameters lead to elements of the 3D model extending beyond the physical constraints or limits of the original design. Together, these four failure cases provide strong evidence that errors in the parameterization of 2D models directly lead to inaccuracies in 3D model reconstruction. Each case illustrates the cascading effect of parameter errors from the 2D representation to the final 3D model, further underscoring the necessity for robust and precise parameterization methods in 2D-to-3D model conversion processes.